Indian Journal of Science and Technology, *Vol 8(19), IPL097, August 2015*
ISSN (Print) : 0974-6846
ISSN (Online) : 0974-5645

Effect of Doping Concentration on the Performance of a Thermally Actuated MEMS Resonator using Piezoresistive Readout

P. A. Ajeesh*, Ribu Mathew and A. Ravi Sankar

School of Electronics Engineering (SENSE), VIT Chennai Campus, VIT University, Chennai-600 127, Tamil Nadu, India; ajeesh15@gmail.com, ribumathew88@gmail.com, a.ravishan@gmail.com

Abstract

Background/Objective: Thermally actuated dog-bone actuators with an in-plane extensional mode of operation and integrated piezoresistive sensing have found versatile applications especially in realizing miniaturized precision oscillators. In this paper, we present a systematic investigation on the impact of dimensional scaling of the resonator structure and the surface doping concentration of the piezoresistor on the performance of a joules heating driven thermal actuator. **Methods/ Statistical Analysis:** To enhance the performance, the dependence of the in-plane resonant frequency and piezoresistive sensing mechanism on the electrical and mechanical design parameters of the actuator has been investigated. Especially, an in-depth analysis of the effect of the dimensional scaling and the surface doping concentration of the piezoresistor on the electromechanical response of the actuator were performed. The resonator structure and the joules heating induced actuation mechanism were efficiently modeled using a Finite Element Model (FEM) software simulation tool IntelliSuite®. **Findings:** Here, we devise a modified version of the thermally actuated dog-bone resonator with enhanced performance compared to the traditional designs reported in the literature. The simulation results show that the modified version of the thermally actuated resonator with an additional central beam depicts an improved in-plane extensional mode of resonant frequency by a factor of 2.55. It has been shown that the surface doping concentration of the piezoresistor plays a crucial role in determining the resonant frequency and the equivalent electrical signal by directly influencing the rate of heat generation by varying the drive current of the actuator. In addition, it has been also demonstrated that the doping concentration also plays an important role in determining the resultant magnitude of $\Delta R/R$ of the thermally driven actuator. **Conclusion/Improvements:** It has been demonstrated that the performance of the thermally actuated resonators improve with dimensional scaling. Moreover, the performance metrics of the thermally driven resonator with piezoresistive readout has been shown to have a strong dependence on the surface doping concentration of the piezoresistor.

Keywords: Dog-bone Actuator, Piezoresistive Readout, Surface Doping Concentration, Thermal Actuation

1. Introduction

Microelectromechanical Systems (MEMS) based resonators constitute an integral module of the modern communication systems[1]. Typical applications of MEMS based resonators include frequency references, filters, sensors, etc. to cite a few. For precision oscillations, micro machined resonators are preferred over the conventional LC based oscillator mainly due to its high Q-factor. Similarly, compared to the generic quartz based designs reported in the literature[2], micro machined resonators with silicon provide advantages of higher level of miniaturization and high degree of integration making the system compact. In addition, they also provide the advantages of superior performance parameters like phase noise response, low power expenditure and minimal temperature drift.

A majority of the earlier reports on MEMS resonators utilize a capacitive[3,4] or piezoelectric[5] electromechanical

*Author for correspondence

transduction method to convert the mechanical deformation to an equivalent electrical signal. In capacitive resonators, the magnitude of the generated electric field is a function of the gap between the capacitor plates[6]. However, for a higher magnitude of the electric field between the plates, the gap between the plates should be in sub-micrometers. Such stringent geometrical design presents numerous fabrication challenges and design issues especially like the squeeze film damping effects due to the trapped air and the fringing electric field lines to name a few. Similarly, piezoelectric resonators need the deposition of a metallic film and a piezoelectric material on the actuator, which reduces its Q-factor[7]. Moreover, the above mentioned transduction mechanisms need a larger electrode area, resulting in an increase in the real estate, and hence limiting the number of devices that can be integrated onto the same chip. Another limitation of the above mentioned transduction methods are the large parasitic capacitance accompanied with these devices.

The thermal actuators have the advantages of low operating voltage, large actuation force and simplicity in design. Thermal actuation coupled with piezoresistive sensing[8] can be implemented in a smaller area giving a performance matching the conventional transduction methods. Literature encompasses various designs of thermally actuated resonators with piezoresistive readout[8-12].

In this paper, we have modeled and designed a modified version of the I²- Bulk Acoustic wave Resonators (I²-BAR) or dog-bone MEMS resonators with thermal actuation and piezoresistive readout for a higher frequency of operation. The main focus of the work is to analyze the effect of the surface doping concentration on the thermally actuated MEMS resonators. A systematic analysis was performed to better understand the impact of the surface doping concentration on the resonator performance using a Computer Aided Design (CAD) software tool IntelliSuite®.

2. Device Working Principle

The resonator structure utilized to realize a high frequency of operation is the dog-bone resonator, better known as the I²-Bulk Acoustic wave Resonator (I²-BAR's). Figure 1 shows the 3-D view of a dog-bone resonator structure. At the centre, the resonator structure has two beams, with its end attached to the proof mass. The mechanical stability to the structure is provided by the supporting pads. The thermal actuation principle depends on the localized joule

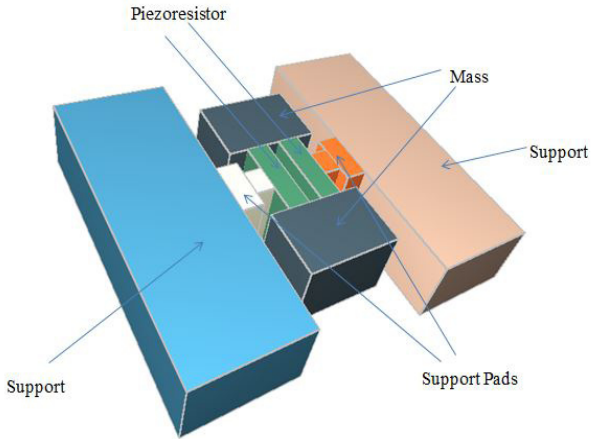

Figure 1. 3-D schematic of the dog-bone thermally actuated resonator with piezoresistive readout[12].

or resistive heating in the structure. The heat generated due to the resistive heating of the structure coupled with the different thermal expansion of the material results in the mechanical deformation in the beams.

Thermal actuation and the equivalent electrical signal from the piezoresistor are obtained by giving an actuation voltage to the pads of the resonator structure. A combination of AC and DC bias voltage is applied to the pads of the resonator. AC voltage is applied to resonate the structure in the desired mode and the DC voltage for obtaining the electrical equivalent of the actuation. Due to the applied voltage and the resultant joules heating, the resonator structure has a non-uniform temperature profile and alternating temperature gradient. The non-uniformity in the temperature profile is due to the difference in the geometry of the structure. Maximum temperature is seen in the proof mass. The alternating temperature gradient is as a result of the swing in the power loss, which ultimately results in the thermal expansion of the extensional beams. The resultant extensional force induces the desired length extensional mode of vibration.

When the resonant frequency of the structure equals the ohmic loss and its resulting temperature fluctuations, then the vibration amplitude of the resonator is amplified by the Q factor of the device. The amplified periodic stress in the beam columns leads to higher variations in the electrical resistance due to the piezoresistance effect. When biased with a DC voltage, the resistance fluctuation modulates the current passing through the device, resulting in an AC component known as the motional current.

2.1 Thermal Actuation

Thermal actuation is accomplished by the energy dissipation phenomenon of the joules heating in the structure when a large current is passed. The combined application of the AC current with the DC bias voltage results in an alternating temperature gradient which translates into an actuating action. The actuating frequency of the structure depends directly on the thermal mass of the resonator structure. A small thermal time constant can be obtained by scaling the device down.

The thermal time constant of the structure is given by the equation $\tau_{th} = R_{th} C_{th}$, where, R_{th} and C_{th} are the thermal resistance and capacitance given by Equation 1 and 2 respectively,

$$R_{th} = \frac{\rho l}{A} \quad (1)$$

where, ρ is the thermal resistivity of the actuator material, l is the length of the actuator element and A is the area of the actuator.

$$C_{th} = 2\beta\rho lw\, C_H \quad (2)$$

where, β is the correction factor with its value ranging from 1.02 to 1.11[13], w is the width of the actuator, and C_H is the specific heat of silicon.

2.2 Piezoresistive Sensing

The mechanical movement of the actuating beams due to the coupled action of the non-uniform temperature profile and the Temperature Coefficient of Expansion (TCE) is due to the ac and dc bias voltages. The deformation in the mechanical structure induces stress, which is converted into an electrical equivalent signal by the integrated piezoresistive readout. The equivalent electrical signal is represented in terms of the parameter ΔR/R, where, R is the nominal resistance and ΔR is the change in the nominal resistance.

3. Proposed Device

The I³-BAR is designed on a Silicon On Insulator (SOI) (100) wafer. The piezoresistors are designed along the <110> direction with selective doping of phosphorus in silicon. A schematic of the thermally driven piezoresistive readout I³- BAR is shown in Figure 2. When the thermal actuation is provided, then the proof mass act as the heat tanks and the beams acts as the actuators.

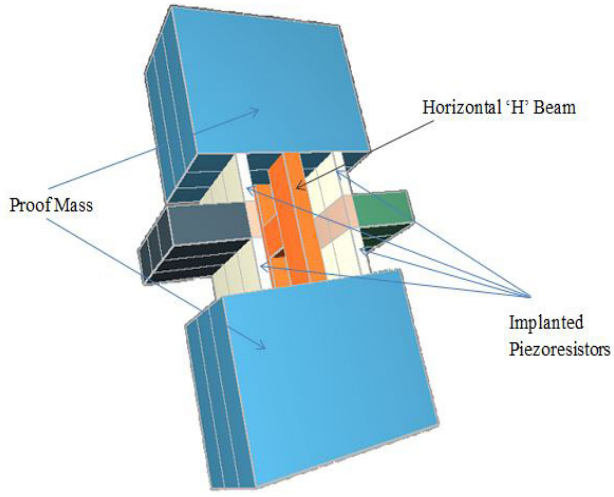

Figure 2. 3-D schematic of the proposed resonator virtually fabricated in the Intellisuite™ software.

Here, the actuator structure itself acts as the sensing piezoresistors for converting the mechanical movement into an equivalent electrical signal.

The structure consists of an additional center beam compared to the already reported structure shown in Figure 1. The H-shaped center beam makes it an I³- shaped structure. The additional beam increases the stiffness of the structure resulting in an increase in the resonant frequency of the structure.

3.1 Thermoelectromechanical Model of the Resonator

The block diagram representation of the thermally actuated resonator with piezoresistor readout is shown in Figure 3. There are three subsystems representing the interdependence of the mechanical, thermal and electrical parameters of the actuator system. When an input voltage is applied to the system, temperature is generated due to the phenomenon of joules heating. The temperature gradient coupled with the TCE of the structure result into

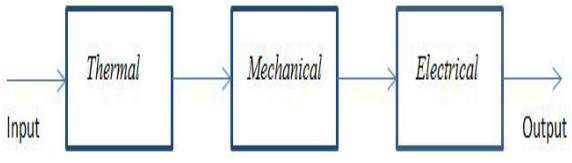

Figure 3. Block diagram of a thermally actuated resonator system with piezoresistive readout.

a desired mechanical movement. Finally, the mechanical movement is transduced into an equivalent electrical signal by the piezoresistor output.

The motional conductance denoted by g_m is defined as the ratio of the motional current to the input ac voltage given by the Equation 3

$$gm = 2Y\alpha Q\pi_l \frac{I_{dc}^2}{C_{th}\omega_0} \quad (3)$$

where, Y is the Young's modulus of silicon, Π_l is the longitudinal piezoresistive coefficient, Q gives the quality factor, l_{dc} is the dc current and ω_0 is the resonant frequency.

The performance of the device is given by the Figure of Merit (FOM) given by Equation 4

$$FOM = \frac{g_m}{P_{DC}} = \frac{2Y\alpha Q\pi_l}{C_{th}\omega_0\left(R_A + R_s\right)} \quad (4)$$

where, P_{DC} is the DC power, R_A is the actuator arm resistance, R_S is the sheet resistance and α is the temperature coefficient of expansion.

4. Simulations

The resonator structures were modelled using various modules of the Finite Element Model (FEM) based Computer Aided Design (CAD) software tool IntelliSuite®. The layout designs were performed in the Blueprint® module. The actuator structures were virtually fabricated and meshed in the 3-D builder module. The thermal, electrical and dynamic analyses were performed using the Thermoelectromechanical® (TEM) tool. Appropriate mechanical, electrical and thermal boundary conditions were applied to analyze the performance of the structure. The microscopic properties of the material utilized in the numerical simulations are summarized in Table 1.

Table 1. Microscale properties of silicon used in simulation

Parameter	Values
Young's Modulus	130 GPa
Poisson	0.278
Density	2330 kg/m^3
CTE	2.6 10^{-6}/°C
Specific heat	700 J kg^{-1}°K^{-1}

5. Results and Discussions

In this section, a detailed analysis of the thermally actuated resonator with piezoresistive readout has been carried out. To better understand the impact of the surface doping concentration of the piezoresistors on the thermally driven actuation mechanism and the resultant equivalent electrical signal, simulations have been carried out. Here, the performance of the proposed resonator structure has been analyzed compared to the reported and the scaled down version of the resonator structures. A systematic study has been carried out to understand the variation in the magnitude and profiles of temperature as a function of the surface doping concentrations of the piezoresistors. In addition, the dependence of the electromechanical response on the surface doping concentration has been also investigated.

It has been observed that, the maximum in-plane displacement of the beam structure in the desired mode is 1 µm as shown in Figure 4. The resonant mode frequency of the structure in the length extensional mode has been evaluated to be 156 MHz.

To understand the impact of the surface doping concentration on the non-uniform temperature profile of the resonator an initial surface doping concentration of 1E19 cm^{-3} is considered. A combination of 3V DC and a 1V AC is applied to the pads of the resonator structure. The non-uniformity in the temperature profile of the resonator is evident as shown in Figure 5. The non-uniformity in the temperature profile is due to the difference in the rate of heat generation of the structure. In addition, the

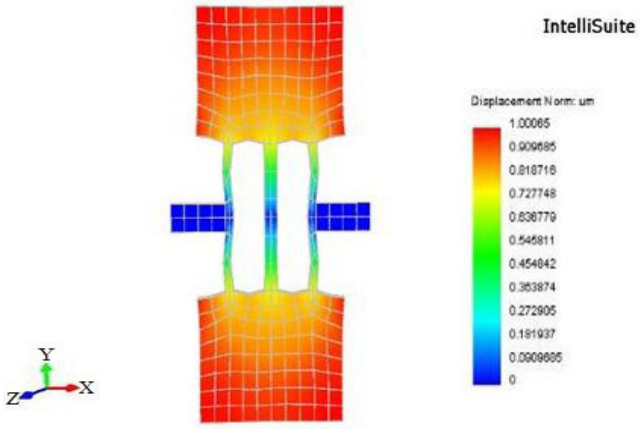

Figure 4. In-plane extensional mode displacement profile of the dog-bone resonator with a resonant frequency of 156 MHz.

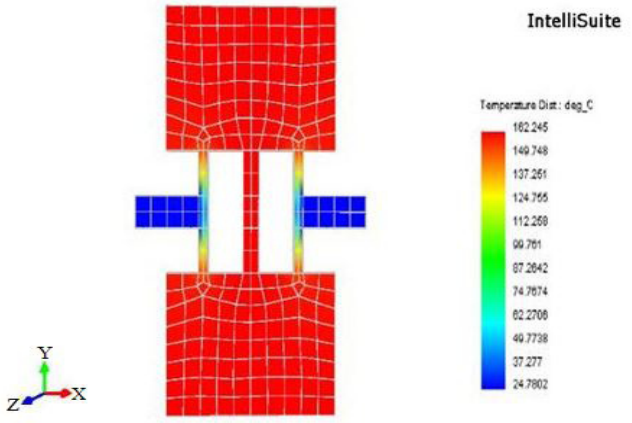

Figure 5. Temperature profile of the modified resonator structure.

AC current also induces a non-uniform temperature distribution. From the figure it is evident that, the proof mass has the maximum temperature, which eventually acts as the heat tanks.

The modified I³-shaped thermally actuated resonator with an additional 'H' beam gives a higher magnitude of vibration (156 MHz). The improvement in the resonant frequency of the structure can mainly be attributed to the increase in the stiffness of the structure due to the additional beam. The electromechanical response of the resonator with variation in the surface doping concentration of the piezoresistor is depicted graphically in Figure 6. With increase in the surface doping concentration there is an increase in the ΔR/R of the resonator due to the increase in the heating induced deformation. However, there is a reduction in the ΔR/R by 63.31%[12], which is due to the additional stiffness introduced by the central beam in the modified structure.

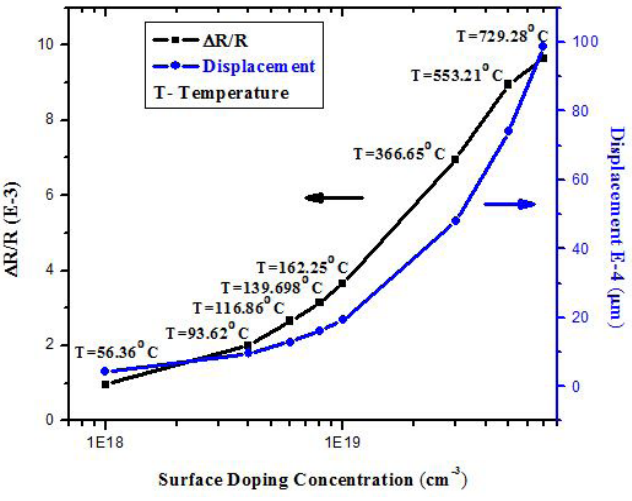

Figure 6. Sensitivity, maximum temperature and displacement as a function of the doping concentration of a 156 MHz modified dog-bone resonator.

Table 2 summarizes the effect of surface doping concentration on the electromechanical response of the resonator. The range of surface doping concentration considered for analysis varies from 1E18 to 7E19 cm^{-3}. The variation in the piezoresistive coefficient (Π_{12}) as a function of the surface doping concentration were calculated from the model proposed by Kanda[14] at room temperature. It is evident that with the reduction in the resistivity due to increase in the doping concentration, the current through the structure increases resulting in an increase in the temperature generated in the structure. Even though, with increase in the surface doping concentration the piezoresistive coefficient reduces, the increase in the temperature is directly translated into a higher magnitude of ΔR/R due to the increase in the mechanical deformation of the structure.

The Figure 7 depicts the variation in the resistivity and the magnitude of current generated in the structure

Table 2. Effect of surface doping concentration on the performance of the modified resonator structure

Surface doping concentration (cm^{-3})	Resistivity (Ω-cm)	Piezo-resistive coefficient (π_{12})[14] (E-11 Pa^{-1})	Maximum temperature (°C)	Displacement E-4 (μm)	ΔR/R (E–3)
1E+18	0.0256	52.866	56.3626	4.39	0.96267
4E+18	0.0117	50.196	93.6225	9.62	2.00378
6E+18	0.00874	49.662	116.863	12.88	2.65621
8E+18	0.00700	46.992	139.698	16.08	3.13712
1E+19	0.00585	45.657	162.245	19.25	3.65195
3E+19	0.00235	34.977	366.652	47.91	6.96369
5E+19	0.00152	29.103	553.213	74.07	8.95569
7E+19	0.00114	23.496	729.284	98.76	9.63837

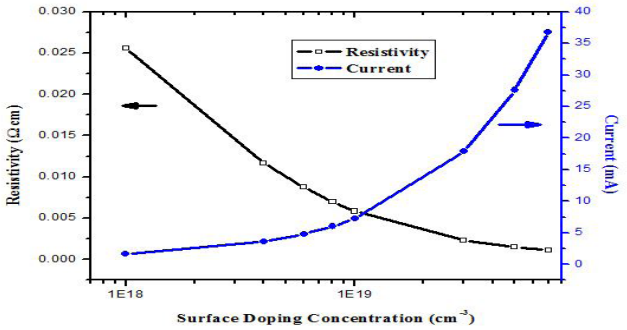

Figure 7. Resistivity and current as a function of the surface doping concentration.

as a function of the surface doping concentration of the piezoresistor. It is evident from figure that as the surface doping concentration increases, the resistivity decreases. Therefore, for a fixed voltage as the surface doping concentration increases, with reduction in resistivity, there is an increase in the magnitude of current in the resonator.

6. Conclusion

This paper explains the design of a modified dog-bone thermally actuated resonator with piezoresistive readout. The proposed design of the resonator with an additional central beam, demonstrated an improvement in the resonating frequency by a factor of 2.55 compared to the conventional dog-bone resonator[12]. To better understand the effect of surface doping concentration on the electromechanical response of the resonator an in-depth analysis has been carried out. It was shown that the surface doping concentration has a direct impact on the joules heating induced maximum temperature on the resonator. To conclude, it was demonstrated that the resultant $\Delta R/R$ of the resonator structure is a function of the surface doping concentration and a higher value of doping is desirable to obtain a higher magnitude of $\Delta R/R$.

7. References

1. Nguyen CTC. MEMS technology for timing and frequency control. IEEE Transactions on Ultrasonics Ferroelectrics and Frequency Control. 2007 Feb; 54(2):251–70.
2. Chang SM, Muramatsu H, Nakamura C, Miyake J. The principle and applications of piezoelectric crystal sensors. Materials Science and Engineering: C. 2000 Aug; 12 (1-2):111–23.
3. Pourkamali S, Ho GH, Ayazi F. Low-impedance VHF and UHF capacitive silicon bulk acoustic wave resonators. IEEE Transactions on Electron Devices. 2007 Aug; 54(8):2017–23.
4. Pourkamali S, Hao Z, Ayazi F. VHF single crystal silicon side supported disk resonators - part ii: implementation and characterization. Microelectromechanical System. 2004 Dec.; 13(6):1054–62.
5. Rinaldi M, Zuniga C, Zuo C, Piazza G. Super-high-frequency Two-port AlN contour mode resonators for RF applications. IEEE Transactions on Ultrasonics Ferroelectrics and Frequency Control. 2010 Jan; 57(1):38–45.
6. Artieda A, Muralt P. High-Q AlN/SiO_2 symmetric composite thin film bulk acoustic wave resonators. IEEE Transactions on Ultrasonics Ferroelectrics and Frequency Control. 2008 Nov; 55(11):2463–8.
7. Piazza G, Stephanou PJ, Pisano AJ. Piezoelectric aluminum nitride vibrating contour-mode MEMS resonators. Journal of Micro electromechanical Systems. 2006 Dec; 15(6):1406–18.
8. Van Beek JTM, Steeneken PG, Giesbers B. A 10MHz piezoresistive mems resonator with high Q. IEEE International Frequency Control Symposium and Exposition; Miami, FL; 2006. p. 475–80.
9. Van Beek JTM, Verheijden GJAM, Koops GEJ, Phan KL, Vander A, Voort C, Van Wingerden J, Ernur BD, Bontemps JJM. Scalable 1.1 GHz fundamental mode piezo-resisitive silicon MEMS resonator. IEEE IEDM International Electron Devices Meeting; Washington, DC. 2007. p. 411–4.
10. Bontemps JJM, Murroni A, Van Beek JTM, Van Den Homberg JATM, Koning JJ, Koops GEJ, Verheijden GJAM, Van Wingerden J, Phan KL, Vermeeren P, Van der Avoort P, Beijerinck HCW, Baltus PGM. 56 MHz piezoresistive micromechanical oscillator. Transducers International Solid-State Sensors, Actuators and Microsystems Conference; Denver, CO; 2009. p. 1433–6.
11. Eloi MF, Munoz-Gamarra JL, Giner J, Uranga A, Barniol N. A 230 MHz CMOS-MEMS bulk acoustic wave resonator. Micro Electronic Engineering. 2012; 98:458–62.
12. Amir R, Siavash P. High frequency thermally actuated electromechaniclal resonators with piezoresistive readout. IEEE Transactions on Electron Devices. 2011 Apr; 58(4):1205–14.
13. Hall HJ, Rahafrooz A, Brown JJ, Bright VM, Pourkamali S. I-shaped thermally actuated VHF resonators with submicron components. Sensors and Actuators A. 2013; 195:160–6.
14. Yozo K. A graphical representation of the piezoresistance coefficients in silicon. IEEE Transcations on Electron Devices. 1982 Jan; 29(1):64–70.